

Hoda Moazzen,¹ Xiangru Lu,¹ Murong Liu,² and Qingping Feng^{1,2,3}

Pregestational Diabetes Induces Fetal Coronary Artery Malformation via Reactive Oxygen Species Signaling



Diabetes 2015;64:1431–1443 | DOI: 10.2337/db14-0190

Hypoplastic coronary artery disease is a congenital coronary artery malformation associated with a high risk of sudden cardiac death. However, the etiology and pathogenesis of hypoplastic coronary artery disease remain undefined. Pregestational diabetes increases reactive oxygen species (ROS) levels and the risk of congenital heart defects. We show that pregestational diabetes in mice induced by streptozotocin significantly increased 4-hydroxynonenal production and decreased coronary artery volume in fetal hearts. Pregestational diabetes also impaired epicardial epithelial-to-mesenchymal transition (EMT) as shown by analyses of the epicardium, epicardial-derived cells, and fate mapping. Additionally, the expression of hypoxia-inducible factor 1 α (*Hif-1 α*), *Snail1*, *Slug*, basic fibroblast growth factor (*bFgf*), and retinaldehyde dehydrogenase (*Aldh1a2*) was decreased and E-cadherin expression was increased in the hearts of fetuses of diabetic mothers. Of note, these abnormalities were all rescued by treatment with *N*-acetylcysteine (NAC) in diabetic females during gestation. Ex vivo analysis showed that high glucose levels inhibited epicardial EMT, which was reversed by NAC treatment. We conclude that pregestational diabetes in mice can cause coronary artery malformation through ROS signaling. This study may provide a rationale for further clinical studies to investigate whether pregestational diabetes could cause hypoplastic coronary artery disease in humans.

Pregestational diabetes is a risk factor for congenital heart defects in infants (1,2). Clinical studies have shown that pregestational diabetes increases the risk of congenital

heart defects in the offspring by three- to fivefold compared with nondiabetic pregnancies (1–3). To date, analysis of congenital heart malformation in the newborn is mainly restricted to major cardiac structures, which include the aorta, pulmonary artery, atrioventricular septum, cardiac valves, and myocardium, but coronary arteries are not routinely examined (4). Congenital malformation can occur in the coronary arteries, leading to null coronary artery or hypoplastic coronary artery disease (5). Although null coronary artery is embryonically lethal, hypoplastic coronary artery disease is a rare congenital coronary abnormality defined by malformation of one or more major branches of the coronary arteries with a marked decrease in luminal diameter and length. Hypoplastic coronary artery disease can be asymptomatic but often is associated with myocardial infarction and sudden cardiac death during intense physical activity (6). However, the etiology and pathogenesis of hypoplastic coronary artery disease remain undefined. Furthermore, it is not known whether pregestational diabetes results in coronary artery malformation in offspring. Isolated cases of congenital coronary artery abnormalities have been identified in infants by autopsy. However, whether the mothers of these infants had pregestational diabetes was not disclosed in these reports (7,8). A large multicenter case-control study showed a significant association between pregestational diabetes and a wide range of congenital heart defects (1). Because coronary arteries were not routinely examined, defects of coronary arteries were not reported in this study. Of note, a recent population-based study reported cases of coronary

¹Department of Physiology and Pharmacology, University of Western Ontario, London, Ontario, Canada

²Lawson Health Research Institute, London Health Sciences Centre, London, Ontario, Canada

³Department of Medicine, University of Western Ontario, London, Ontario, Canada

Corresponding author: Qingping Feng, qfeng@uwo.ca.

Received 3 February 2014 and accepted 15 November 2014.

This article contains Supplementary Data online at <http://diabetes.diabetesjournals.org/lookup/suppl/doi:10.2337/db14-0190/-/DC1>.

© 2015 by the American Diabetes Association. Readers may use this article as long as the work is properly cited, the use is educational and not for profit, and the work is not altered.

artery anomaly in infants born to mothers with obesity; however, mothers with established diabetes were excluded from this study (9).

Coronary arteries are developed from several sources of progenitors, which include endothelial cells of the sinus venosus, proepicardial organ, and endocardium (10–12). Current understanding is that cells from the proepicardial organ migrate toward the myocardium and form the epicardium. Concurrent with formation of the epicardium, some epicardial cells undergo epithelial-to-mesenchymal transition (EMT), migrate to the subepicardial space and myocardium, and become epicardial-derived cells (EPDCs). Simultaneously, a subpopulation of endothelial cells of the sinus venosus also migrates to the subepicardial space, forming subepicardial endothelial progenitors (11). When they reside in the myocardium, the EPDCs give rise to vascular smooth muscle cells and fibroblasts (13), whereas subepicardial endothelial progenitors give rise to coronary endothelial cells (14). Together, EPDCs and subepicardial endothelial cells contribute to the development of coronary arteries with a minor contribution from the endocardium.

Epicardial EMT is regulated by several epicardial transcription factors and myocardial-induced signaling molecules (15). An important factor in vasculogenesis and heart development is hypoxia-inducible factor 1 α (HIF-1 α) (16), which regulates many downstream target genes, including Wilms tumor 1 (Wt1), a critical transcription factor expressed in epicardial progenitors and EPDCs (17,18). Studies have shown that Wt1 directs epicardial progenitors to become smooth muscle cells and fibroblasts and forms coronary arteries (19). Pregestational diabetes increases reactive oxygen species (ROS) production (20,21) and downregulates HIF-1 α expression in embryos (22). We have shown that treatment with *N*-acetylcysteine (NAC) increases reduced glutathione (GSH) levels and decreases ROS production in the hearts of fetuses of mice with pregestational diabetes (20). The current study tested the hypothesis that pregestational diabetes impairs epicardial EMT and induces coronary artery malformation in offspring. We further hypothesized that these abnormalities are mediated by ROS signaling and can be rescued by NAC treatment in diabetic females during gestation.

RESEARCH DESIGN AND METHODS

Animals

C57BL/6J wild-type *Wt1*^{CreERT2/+} and *Rosa26*^{mTmG} mice were purchased from The Jackson Laboratory (Bar Harbor, ME). Animals were handled in accordance with the National Institutes of Health *Guide for the Care and Use of Laboratory Animals* (NIH publication no. 85-23, revised 1996). All procedures involving mouse handling and manipulation were in accordance with the guidelines of the Canadian Council of Animal Care and approved by the Animal Use Subcommittee at the University of Western Ontario.

Induction of Diabetes and NAC Treatment

Eight-week-old C57BL/6 female mice were induced to become diabetic by streptozotocin (STZ) 80 mg/kg body weight/day i.p. injections for 3 consecutive days as described previously (20,23,24). STZ was dissolved in sodium citrate (pH 4.0), and mice treated with sodium citrate served as controls. Nonfasting blood glucose levels were determined 1 week after STZ injection using a glucose meter (OneTouch Ultra2; LifeScan Canada, Burnaby, BC). Mice with blood glucose levels >11 mmol/L were considered diabetic and bred with normal adult males. Vaginal plugging was monitored as a sign of successful mating, and the day of vaginal plugging was recorded as day 0.5 of gestation (E0.5). A subgroup of control and diabetic mice received 4 mg/mL NAC in drinking water from E0.5 to the end of gestation or harvesting of the embryos (20). Water and food intake of pregnant mice was measured and normalized to body weight.

Fate Mapping Analysis

Fate mapping of the *Wt1*⁺ lineage was performed using *Wt1*^{CreERT2/+} (Stock #10912, The Jackson Laboratory) and the double-fluorescent Cre reporter line *Rosa26*^{mTmG} (Stock #7576). *Wt1*^{CreERT2/+} is a heterozygous *Wt1*^{-/+} mouse, where exon 1 of the *Wt1* gene is deleted and replaced by a *CreERT2* sequence under the control of the *Wt1* promoter (19). *CreERT2* is created by fusion of Cre recombinase to a modified human estrogen receptor ligand-binding domain (ERT2). The *Rosa26*^{mTmG} reporter mice possess *loxP* sites on either side of a membrane-targeted tomato (mT) cassette followed by a membrane-targeted green fluorescent protein (GFP) (mG) cassette. In the absence of Cre, mT (red fluorescence) is expressed in all tissues. In the presence of Cre, the mT cassette is deleted and mG (green fluorescence) expressed only in the targeted cells. Female *Rosa26*^{mTmG} mice were induced to become diabetic by STZ 80 mg/kg body weight/day i.p. for 3 days as already described and were bred with *Wt1*^{CreERT2/+};*Rosa26*^{mTmG} males. Tamoxifen 50 mg/kg body weight i.p. was injected into diabetic or control females at E10.5. Upon tamoxifen administration, Cre is activated in *Wt1*-expressing cells and induces recombination to express GFP, which is one of the two fluorescent proteins in the *Wt1*^{CreERT2/+};*Rosa26*^{mTmG} offspring. Embryos were harvested at E14.5. Double-transgenic *Wt1*^{CreERT2/+};*Rosa26*^{mTmG} embryos were sectioned and immunostained for GFP. The *Wt1*⁺ derivatives, which are GFP⁺ cells and structures, were quantified and compared between the offspring of diabetic and control mice.

Analysis of 4-Hydroxynonenal Production

To assess oxidative stress, embryonic heart tissues were harvested at E14.5. Frozen samples were cut into 10- μ m sections using a cryostat (CM1950; Leica). Heart sections were stained with 4-hydroxynonenal (4-HNE) antibody (1:300; abm Inc.) followed by CY3-conjugated anti-goat IgG (1:1,000; Jackson ImmunoResearch). 4-HNE fluorescence signals were detected using a fluorescence microscope

Table 1—Nonfasting maternal blood glucose levels, water and food intake during gestation, and incidence of CAM and CHD in fetuses from E16.5 to E18.5

	Control	Diabetes	Control + NAC	Diabetes + NAC
Pregnant mice (<i>n</i>)	8	10	8	10
Blood glucose at E0.5 (mmol/L)	6.9 ± 0.3	17.2 ± 1.6*	7.5 ± 0.3	14.9 ± 1.0*
Blood glucose at E10.5 (mmol/L)	8.6 ± 0.5	24.2 ± 2.2*	8.9 ± 0.5	22.0 ± 1.4*
Pregnant mice (<i>n</i>)	12	15	13	13
Daily water intake (mL/20 g BW)	3.0 ± 0.1	23.0 ± 3.8*	3.0 ± 0.2	5.8 ± 0.6*†
Daily food intake (g/20 g BW)	3.8 ± 0.1	6.0 ± 0.6*	4.0 ± 0.2	3.4 ± 0.2†
Litters (<i>n</i>)	3	4	3	4
CAM/total fetuses (<i>n/N</i>)	0/26	13/28*	0/25	2/34†
CHD/total fetuses (<i>n/N</i>)	0/26	17/28*	0/25	2/34†
CHD + CAM/total fetuses (<i>n/N</i>)	0/26	11/28	0/25	1/34†
CAM (%)	0	46	0	6
CHD (%)	0	61	0	6
CHD + CAM (%)	0	39	0	3

Data are mean ± SEM unless otherwise indicated. Blood glucose levels were analyzed by one-way ANOVA followed by Newman-Keuls test. A χ^2 analysis was used to compare the incidence of CAM and CHD. BW, body weight; CAM, coronary artery malformation; CHD, congenital heart defect, which includes ventricular septal defect, atrioventricular septal defect, transposition of great arteries, and double-outlet right ventricle. * $P < 0.01$ vs. respective controls. † $P < 0.01$ vs. diabetes.

(Observer D1; Zeiss, Oberkochen, Germany). At least five images were captured using a fixed exposure time for each heart, and intensities of fluorescence signals per myocardial area were quantified using AxioVision software (Zeiss).

Immunohistochemistry

Immunohistochemical analysis was performed to study the formation of the coronary vasculature and its precursors. In brief, the thorax of fetuses and neonates were harvested and processed in 4% paraformaldehyde overnight, embedded in paraffin, and sectioned transversely in 5- μ m sections. Before immunostaining, antigen retrieval was performed in citric acid buffer (0.01 mol/L, pH 6.0) for 12 min at 94°C using a microwave oven (BP-111; Microwave Research & Applications, Inc., Carol Stream, IL). Samples were incubated with primary antibody overnight, as follows: anti- α -smooth muscle actin (1:3,000, Sigma-Aldrich), biotinylated lectin-1 (1:250, Vector Laboratories), anti-Wt1 (1:300, Calbiochem), anti-E-cadherin (1:200, Santa Cruz), anti-GFP (1:1,000, Abcam), anti-phosphohistone H3 (pHH3) (1:500, Abcam), and anticleaved caspase-3 (1:800, Cell Signaling) followed by one of the following secondary antibodies (Vector Laboratories) for 1 h: biotinylated goat anti-rabbit IgG (1:500), biotinylated goat anti-mouse IgG (1:500), or biotinylated donkey anti-goat IgG (1:500). Signals were amplified by incubation with avidin/biotin complex reagent (Vector Laboratories) and visualized using 3-3'-diaminobenzidine tetrahydrochloride (Sigma-Aldrich). Heart sections were counterstained with hematoxylin (Thermo Scientific), and images were captured using a light microscope (Observer D1; Zeiss). To visualize and analyze coronary artery volume, images of every 25- μ m heart section immunostained

with α -smooth muscle actin were captured and imported into the Amira software program for three-dimensional reconstructions. Using the analytical tools of Amira, pixels were converted to volume (μ L), and a ratio of coronary artery volume to myocardial volume was obtained.

Ex Vivo Heart Explant Culture

EMT was assessed ex vivo. Ventricles of E12.5 embryos from control dams were harvested and cultured on collagen gel (25). Collagen (1 mg/mL, type I collagen of rat's tail; BD Bioscience) was prepared in M199 media (M5017; Sigma) containing 5 mmol/L D-glucose or in M199 media with an additional 25 mmol/L D-glucose, making the final D-glucose concentration 30 mmol/L. Casted collagen was hydrated by Opti-MEM media plus 1% FBS and insulin-transferrin-selenium for 30 min at 37°C. E12.5 ventricles were explanted and incubated at 37°C overnight. The following day, 5 or 30 mmol/L D-glucose in M199 media with 10% FBS were added to the heart explants. The glucose concentration was ~5 mmol/L higher than the blood glucose of diabetic dams at E10.5. Heart explant cultures were treated with or without 0.5 mmol/L NAC. The number of spindle-shaped cell outgrowths from the explanted ventricles was quantified 4 days post-culturing. Images were captured using a phase contrast microscope (Zeiss).

Real-Time RT-PCR

Total RNA was extracted from individual E11.5 fetal hearts using RNeasy Mini Kit (QIAGEN, Burlington, ON) per the manufacturer's instructions. cDNA was synthesized from 0.1 μ g total RNA using Maloney murine leukemia virus reverse transcriptase in 10 μ L reactions, which were diluted by three times for genes of interest and 500 times

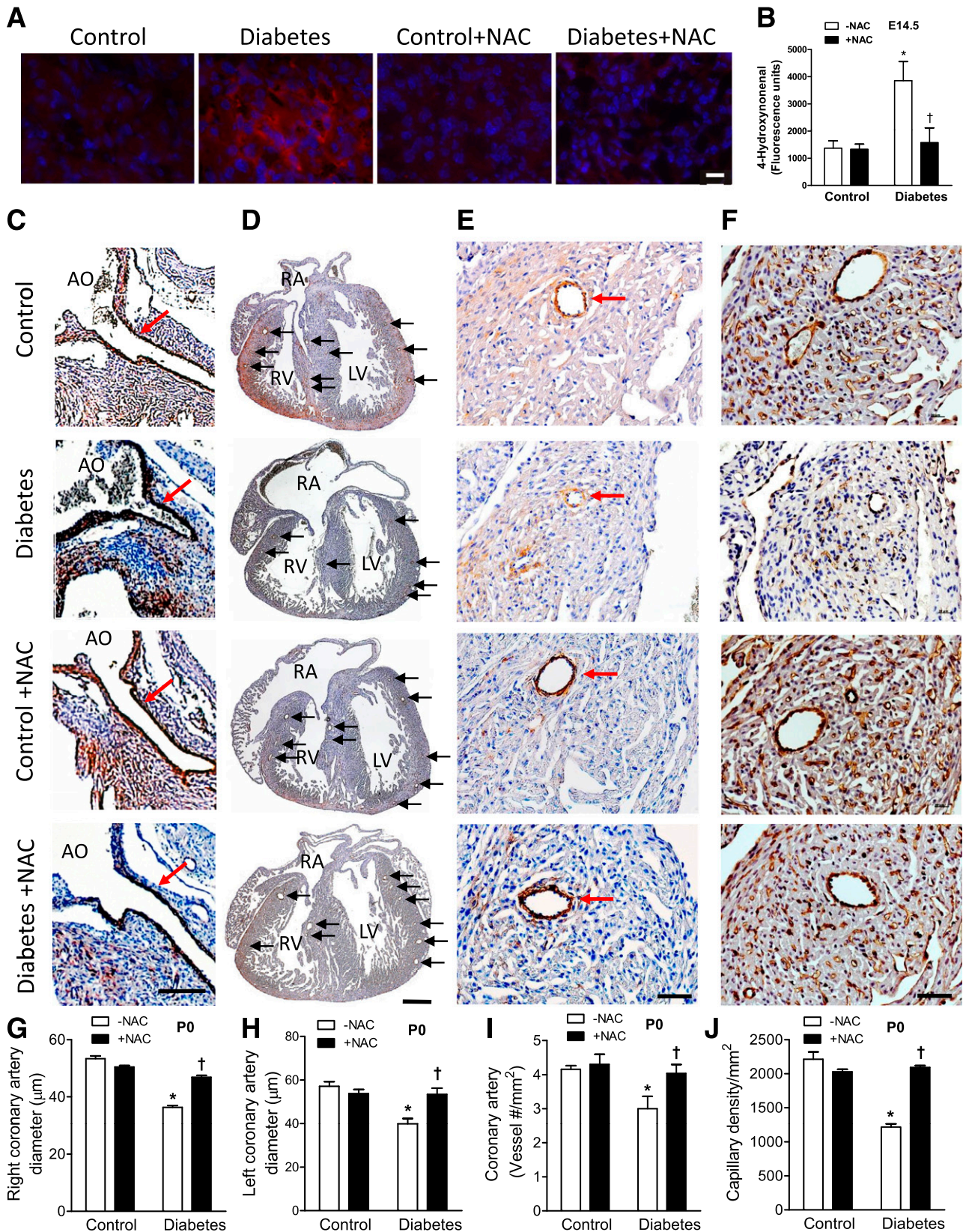


Figure 1—4-HNE production and histological analysis of coronary arteries. **A**: Representative images of 4-HNE immunostaining in E14.5 hearts. **B**: Quantification of 4-HNE immunofluorescence per myocardial area ($n = 4$ neonatal hearts from two to three litters per group). Smooth muscle and endothelial cells were marked by α -smooth muscle actin (**C–E**) and lectin 1 (**F**) immunostaining (brown), respectively. Data in **C–J** are from P0 hearts. **C**: Representative images of left-side main coronary artery branch at the aortic root. **D**: Representative images of coronary artery branches in the myocardium. Arrows point to the coronary vessels. **E**: Coronary artery vessels in the myocardium. **F**: Capillaries in the myocardium. **G** and **H**: Diameters of the left- and right-side coronary arteries at the aortic root ($n = 12$ –15 hearts/

for housekeeping gene 28S. Two microliters diluted cDNA were used for real-time PCR amplification using EvaGreen qPCR MasterMix (Applied Biological Materials, Vancouver, BC). Specific primers were designed for *Hif-1 α* , *Snail1*, *Slug*, basic fibroblast growth factor (*bFgf*), β -catenin, and *Aldh1a2* (Supplementary Table 1). Samples were amplified for 35 cycles using Eppendorf realplex (Eppendorf, Hamburg, Germany). The mRNA levels in relation to 28S rRNA were determined (25).

Statistical Analysis

Data are presented as mean \pm SEM. Statistical analysis was performed using one-way ANOVA followed by Newman-Keuls test (GraphPad Prism version 3.0 software). The incidence of malformation was assessed by χ^2 test. $P < 0.05$ was considered statistically significant.

RESULTS

Maternal Blood Glucose Levels, Food and Water Intake, and Incidence of Coronary Artery Malformations in Offspring

To examine the effect of pregestational diabetes on coronary artery formation, adult female mice were induced to become diabetic by STZ, and their nonfasting blood glucose levels were determined during gestation. The data show that blood glucose levels in diabetic females were significantly higher than that in normal controls ($P < 0.01$) (Table 1). NAC treatment did not significantly alter blood glucose levels in the diabetic and normal dams. Incidence of coronary artery malformation among fetal hearts of mice with pregestational diabetes was 46%, which was decreased to 6% by NAC treatment ($P < 0.01$) (Table 1). Food and water intake in the diabetic females was about eight times higher than that in control mice. Following NAC treatment, food consumption was similar between control and diabetic mice. However, water intake in the NAC-treated diabetic mice was still twice the amount in control mice ($P < 0.05$) (Table 1). The estimated daily dose of NAC was 0.6 and 1.2 g/kg in control and diabetic mice, respectively.

Pregestational Diabetes Increases Oxidative Stress in Fetal Hearts

We recently showed that superoxide generation is increased in E12.5 fetal hearts of mice with pregestational diabetes, which is normalized by treatment with NAC in drinking water in the diabetic dams during gestation (20). To further assess oxidative stress, immunostaining of 4-HNE, a product of lipid peroxidation (26), was performed in E14.5 hearts (Fig. 1A). Myocardial 4-HNE levels were significantly increased in the offspring of pregestational diabetic mice, which was abrogated by NAC

treatment (Fig. 1B). These data suggest that pregestational diabetes increases ROS and oxidative stress in the fetal heart, which are effectively inhibited by NAC treatment.

Coronary Artery Malformation in Fetal Hearts of Mice With Pregestational Diabetes

Formation of the coronary artery and capillaries was evaluated following immunostaining of α -smooth muscle actin and lectin-1, respectively. Offspring of diabetic mothers showed reduced left- and right-side coronary artery diameter and abundance at postnatal day 0 (P0) (Fig. 1C–E, G–I) and at E16.5 (data not shown). Additionally, coronary arteries in the offspring of diabetic mice had fewer smooth muscle cells surrounding the vessels (Fig. 1E) and decreased capillary abundance at P0 (Fig. 1F and J). Of note, abnormalities in coronary artery and capillary development in the offspring of diabetic mice were rescued by NAC treatment (Fig. 1C–J). Impaired coronary artery development is illustrated in three-dimensional reconstructions of coronary arteries, which demonstrate smaller arteries with reduced arborization in the offspring of diabetic mice at E16.5 and P0 (Fig. 2A). The impaired coronary artery development was not a result of changes in myocardial volume because the ratio of total coronary artery volume to myocardial volume was decreased in the offspring of diabetic mice at P0 and E16.5 (Fig. 2B and C).

Pregestational Diabetes Impairs Epicardial EMT in Fetal Hearts

To gain a better understanding of cellular and molecular events that caused coronary artery malformation in the offspring of diabetic mice, the epicardium and proepicardial organ were studied during embryogenesis using immunohistochemistry to detect Wt1 as a marker. The data show that the epicardium in fetal hearts of pregestational diabetic mice formed a sparse and loosely attached cell layer to the myocardium with significant reductions in the number of Wt1⁺ epicardial and subepicardial cells at E12.5 (Fig. 3A, D, and E). Impaired Wt1 expression in fetal hearts of diabetic mothers was persistent at E14.5, as evidenced by a reduced number of Wt1⁺ cells in the epicardial cell layer and in the compact myocardium (Fig. 3B, F, and G). Concurrent with reductions in the number of epicardial Wt1⁺ cells, the number of E-cadherin-positive epicardial cells was increased in fetal hearts of diabetic mothers at E12.5 (Fig. 3C and H). Of note, NAC treatment during gestation reduced epicardial E-cadherin expression and restored the number of Wt1⁺ cells in the epicardium, subepicardium, and myocardium in fetal hearts (Fig. 3A–H).

group). I: Coronary artery abundance per square millimeter of myocardium ($n = 7$ –10 hearts/group). J: Capillary density per square millimeter of myocardium ($n = 5$ hearts/group). Data in G–J were collected from three to five litters per group. * $P < 0.01$ vs. untreated control; † $P < 0.01$ vs. untreated diabetes. AO, aorta; LV, left ventricle; RA, right atrium; RV, right ventricle. Scale bars are 10 μ m in A; 50 μ m in C, E, and F; and 400 μ m in D.

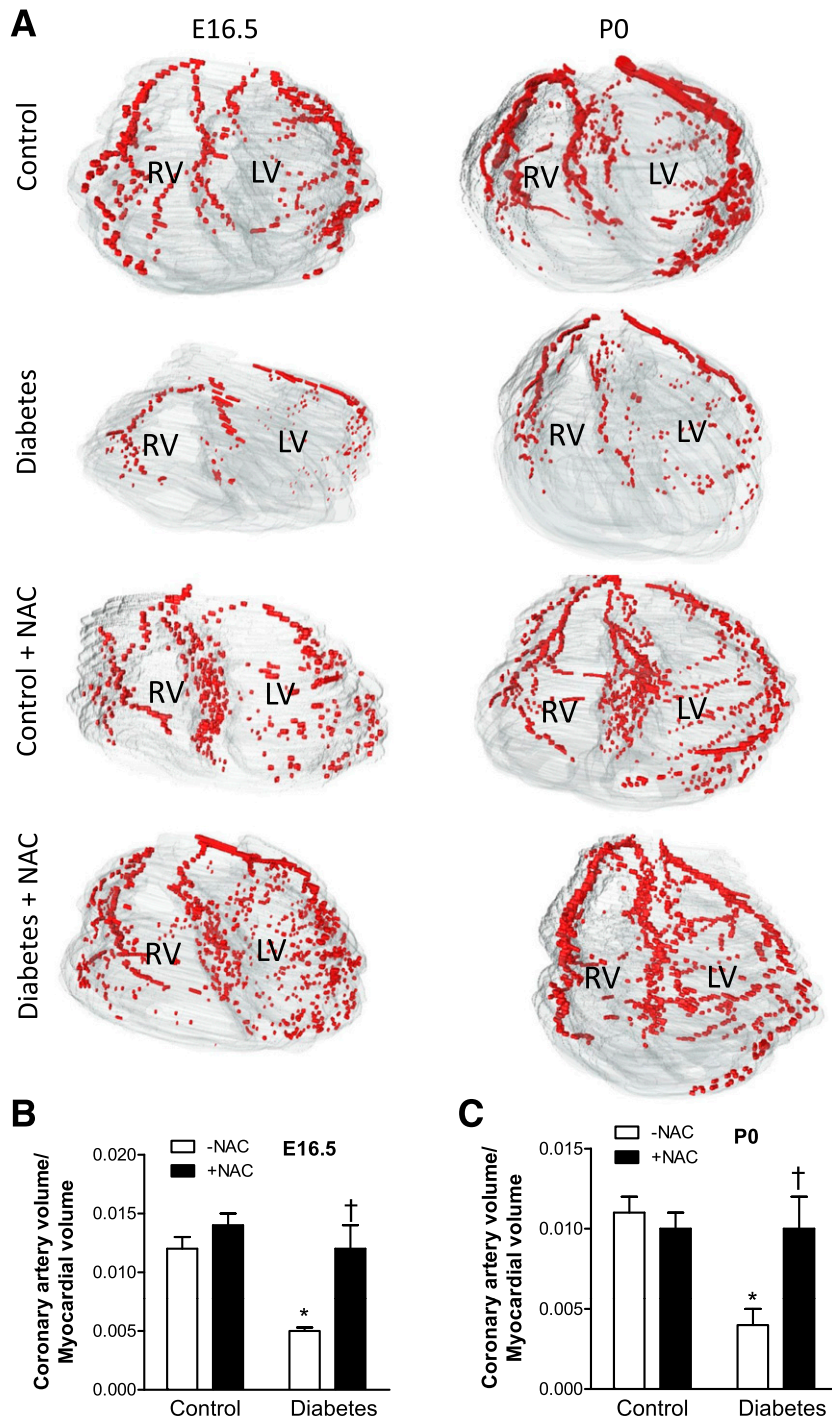


Figure 2—Analysis of coronary artery tree at E16.5 and P0 by three-dimensional reconstructions. *A*: Illustrations of three-dimensional reconstructions of coronary arteries. *B* and *C*: Quantification of the total coronary artery volume normalized to myocardial volume at E16.5 and P0, respectively ($n = 5$ hearts from three litters per group). * $P < 0.05$ vs. untreated control; † $P < 0.01$ vs. untreated diabetes. LV, left ventricle; RV, right ventricle.

However, pregestational diabetes did not alter the number of $Wt1^+$ cells in the proepicardial organ at E9.5 (Fig. 3J).

To directly evaluate the derivatives of epicardial $Wt1^+$ cells, fate mapping analysis was performed using $Rosa^{mTmG}$ female mice in which diabetes was induced by

STZ and then bred to tamoxifen-inducible $Wt1^{CreERT2/+}; Rosa^{mTmG}$ males. Following tamoxifen treatment in the female mice at E10.5, $Wt1^+$ derivatives, including coronary vessels, were observed in the hearts of $Wt1^{CreERT2/+}; Rosa^{mTmG}$ embryos at E14.5 (Fig. 3J). In agreement with our hypothesis, pregestational diabetes diminished $Wt1^+$

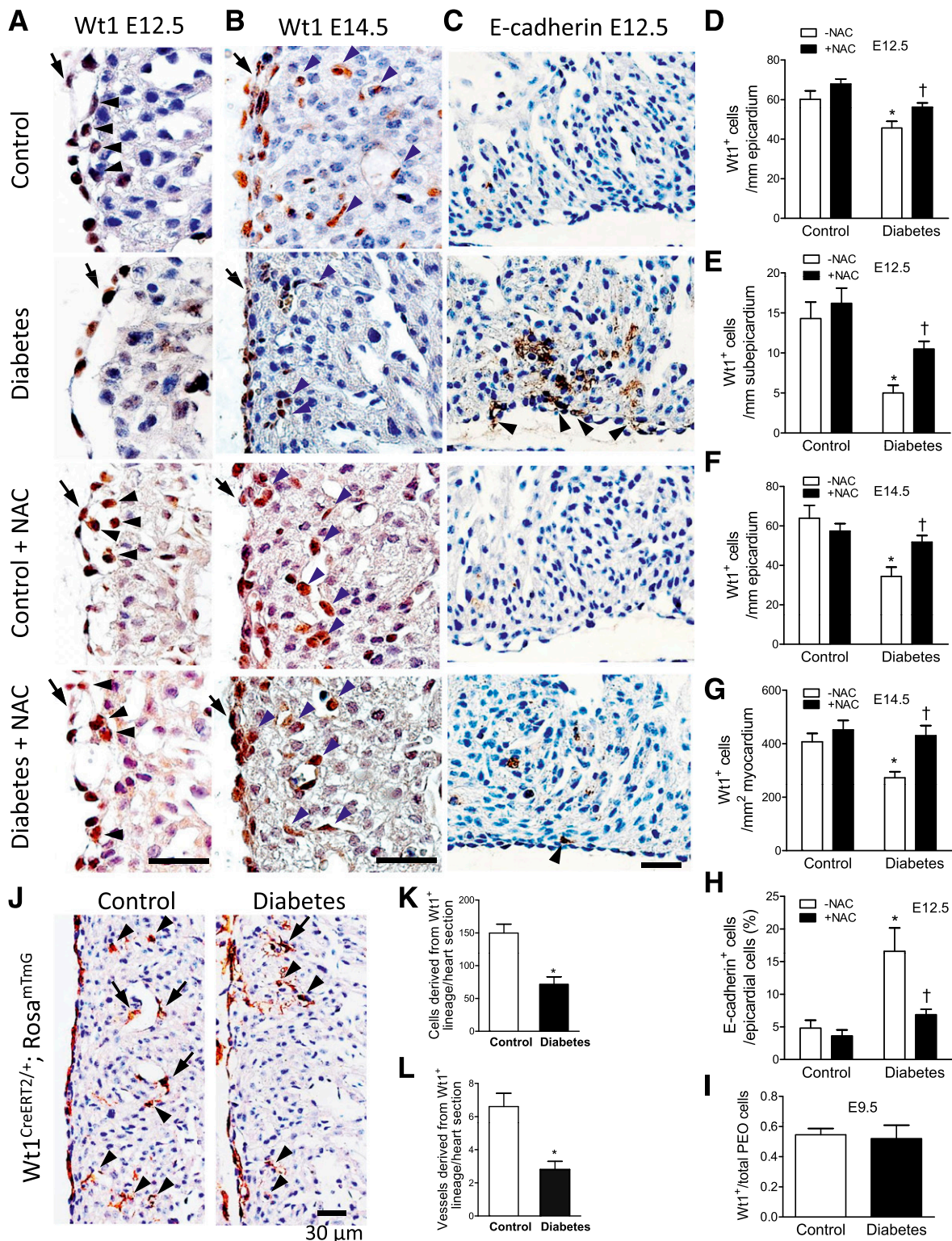


Figure 3—Analysis of the epicardium and fate mapping of Wt1⁺ lineage in the fetal hearts of diabetic dams. *A* and *B*: Representative heart sections of Wt1 immunostaining at E12.5 and E14.5, respectively. Arrows point to the epicardium in *A* and arrow heads point to Wt1⁺ cells in the subepicardium and myocardium in *A* and *B*, respectively. *C*: Representative heart sections of E-cadherin immunostaining at E12.5. Arrow heads indicate E-cadherin-positive epicardial cells. *D* and *E*: Quantification of Wt1⁺ epicardial and subepicardial cell numbers, respectively. *F* and *G*: Quantification of Wt1⁺ cells in the epicardium and myocardium, respectively. *H*: Quantification of E-cadherin-positive cells to total epicardial cell ratio (%). *I*: Wt1⁺ cells in the proepicardial organ (PEO) at E9.5. (Immunostaining images are not shown.) *J*–*L*: Fate mapping of Wt1⁺ lineage. *J*: Representative images of GFP staining in Wt1^{CreERT2/+}; Rosa^{mTmG} E14.5 heart sections of control and diabetic mice. Brown color marks cells (arrowheads) and vessels (arrows) derived from Wt1⁺ lineage. *K* and *L*: Quantification of cells and vessels derived from Wt1⁺ lineage in the myocardium, respectively. *n* = 5–6 hearts from three litters per group. **P* < 0.01 vs. control or untreated control; †*P* < 0.01 vs. diabetes or untreated diabetes.

lineage and coronary vessels in the hearts of *Wt1^{CreERT2/+}; Rosa^{mTmG}* embryos (Fig. 3J–L).

ROS-DEPENDENT DOWNREGULATION OF HIF-1 α SIGNALING IN FETAL HEARTS OF DIABETIC DAMS

To further understand ROS signaling in epicardial EMT, the expression of *Hif-1 α* , a master regulator of vasculogenesis and epicardial EMT (27), and its downstream signaling molecules essential for coronary development were evaluated by RT-PCR. The expression of *Hif-1 α* was significantly diminished in E11.5 fetal hearts of diabetic dams (Fig. 4A). Additionally, mRNA levels of *Snail1* and *Slug*, which are key regulators of EMT, were significantly decreased in fetal hearts of diabetic dams (Fig. 4B and C). Furthermore, retinoic acid signaling may be impaired in the fetal hearts of diabetic dams as evidenced by reduced mRNA levels of *Aldh1a2*, which encodes the retinoic acid

synthesis enzyme retinaldehyde dehydrogenase 2 (RALDH2) (28) and its downstream target *bFGF* (Fig. 4D and E). Of note, these changes in the expression of *Hif-1 α* , *Snail1*, *Slug*, *Aldh1a2*, and *bFGF* were restored in the hearts of offspring of diabetic females by NAC treatment (Fig. 4A–E). However, β -catenin mRNA levels were not significantly altered by pregestational diabetes or NAC treatment (Fig. 4F).

HIGH GLUCOSE IMPAIRS EPICARDIAL EMT EX VIVO

To investigate whether hyperglycemia impairs epicardial EMT in fetal hearts of diabetic mothers, E12.5 hearts were cultured on collagen gel in both high glucose (30 mmol/L) and normal glucose (5 mmol/L) conditions for 4 days (Fig. 5A). The number of spindle-shaped cells, which are epicardial cells that had undergone EMT, was quantified. The data show that the number of spindle-shaped cells was significantly decreased in high-glucose compared

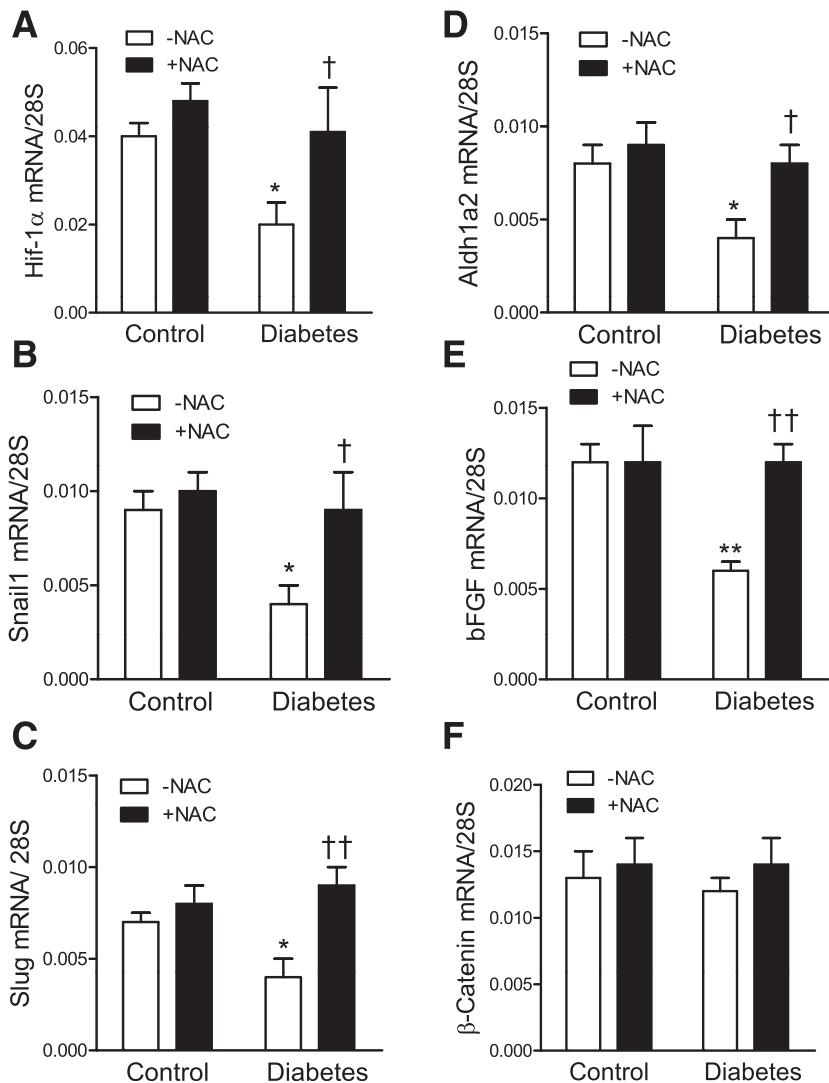


Figure 4—Gene expression of HIF-1 α and its downstream targets critical to epicardial EMT in E11.5 hearts. mRNA levels were analyzed by real-time PCR. A: HIF-1 α . B: *Snail1*. C: *Slug*. D: *Aldh1a2*. E: *bFGF*. F: β -Catenin. * $P < 0.05$, ** $P < 0.01$ vs. untreated control; † $P < 0.05$, †† $P < 0.01$ vs. untreated diabetes (n = 7–9 hearts from three to four litters per group).

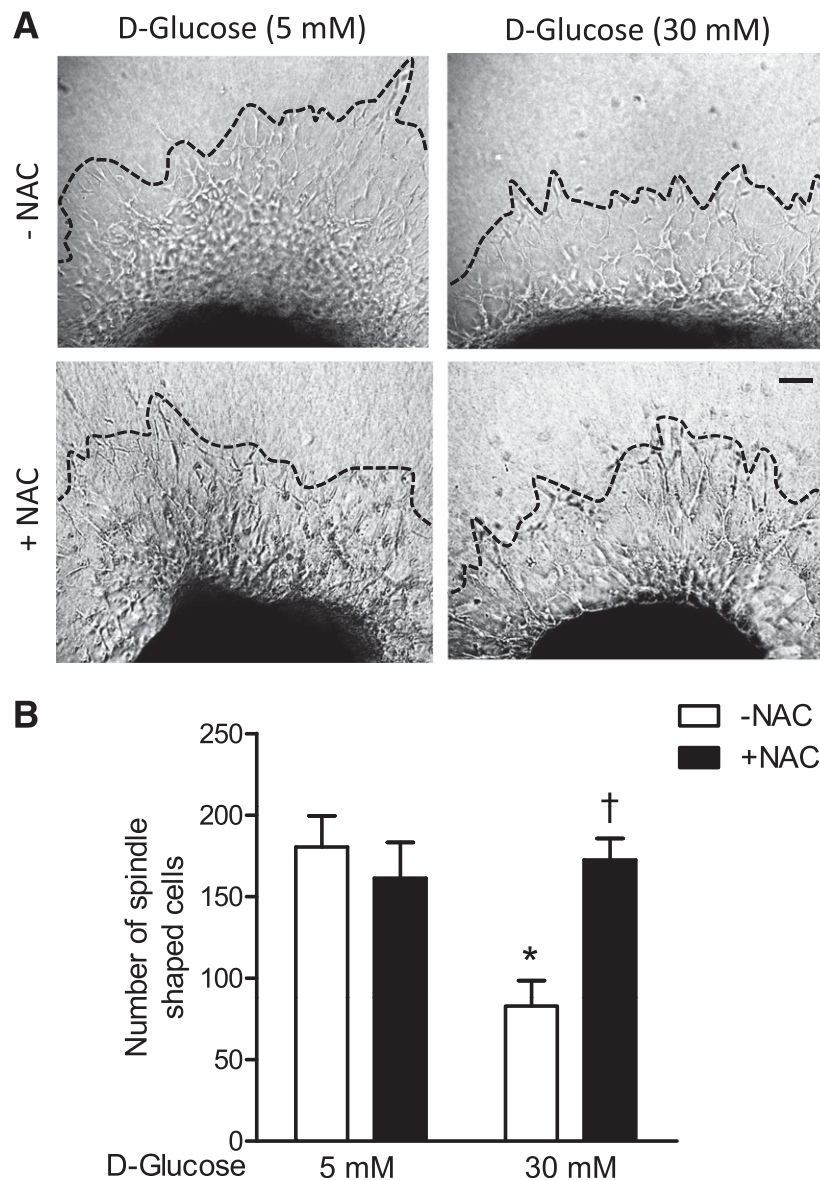


Figure 5—High glucose inhibits EMT ex vivo. *A*: Representative images of ex vivo E12.5 heart explant culture. Dashed line shows the border of migrated cells. *B*: Quantification of the number of spindle-shaped cells, which are cells that have undergone EMT. Scale bar = 50 μm . * $P < 0.01$ vs. untreated control (5 mmol/L D-glucose); † $P < 0.01$ vs. untreated high glucose (30 mmol/L) ($n = 10$ – 12 hearts per group from four litters).

with normal-glucose cultures. The response was restored by NAC 0.5 mmol/L treatment (Fig. 5A and B).

Pregestational Diabetes Diminishes Epicardial Cell Proliferation in Fetal Hearts

To assess the effect of pregestational diabetes on epicardial cell proliferation, immunostaining for pHH3, a marker of mitotic cells, was performed in fetal hearts. The results show that the number of pHH3⁺ epicardial cells was significantly decreased in fetal hearts of diabetic dams at E12.5 and E14.5 (Fig. 6A–D). Of note, treatment with NAC in diabetic dams completely restored epicardial cell proliferation at both time points (Fig. 6C and D). Assessment of the apoptotic epicardial cells in E12.5 hearts using immunostaining

for cleaved caspase-3 show no significant difference between the control offspring ($0.37 \pm 0.16\%$) and the offspring of diabetic mice ($0.33 \pm 0.12\%$, $n = 8$ – 10 hearts/group).

DISCUSSION

The current study demonstrates for the first time to our knowledge that pregestational diabetes impairs development of the coronary artery vasculature in fetal hearts in an animal model. We further demonstrate that pregestational diabetes increases oxidative stress, diminishes HIF-1 α and Wt1 expression, and decreases Snail/Slug and RALDH2/bFGF signaling pathways, leading to the

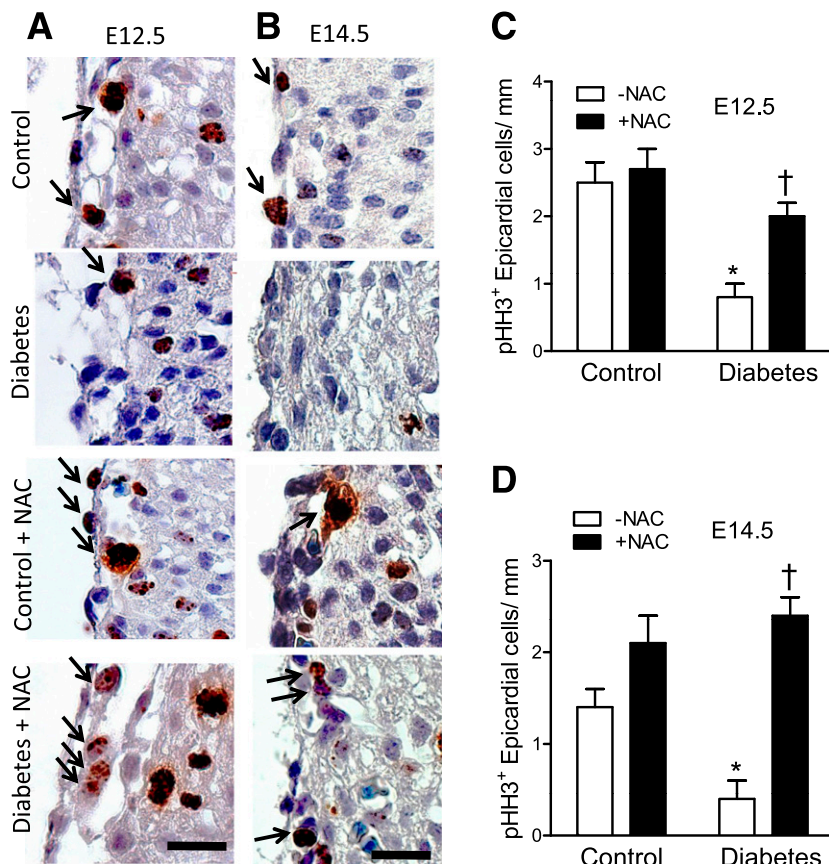


Figure 6—Epicardial cell proliferation. *A* and *B*: Representative images of immunostaining of pHH3 (brown) in E12.5 and E14.5 hearts, respectively. pHH3⁺ epicardial cells are indicated by arrows. *C* and *D*: Quantification of pHH3⁺ epicardial cells per millimeter epicardium ($n = 6$ –8 hearts from three litters per group). Scale bar = 20 μm . * $P < 0.05$ vs. untreated control; † $P < 0.01$ vs. untreated diabetes.

disruption of epicardial EMT and malformation of fetal coronary arteries (for a schematic diagram of the proposed pathway, see Fig. 7). Of note, inhibition of ROS production by NAC restores epicardial EMT and prevents malformation of coronary arteries in the fetal hearts of mice with pregestational diabetes. The study suggests a critical role of ROS signaling in coronary artery malformation during pregestational diabetes.

The embryonic epicardium is a major contributor to coronary artery development (29,30). In this regard, cells from the epicardium undergo EMT and become EPDCs, which then differentiate into vascular smooth muscle cells and cardiac fibroblasts, leading to the formation of coronary vessels. To study whether pregestational diabetes affects epicardial formation, immunohistochemical analysis was performed. Although there were no significant changes in proepicardial organ progenitor cell numbers, the number of epicardial cells was reduced, and the epicardium was detached from the myocardium with decreases in epicardial cell proliferation at E12.5 and E14.5 in the hearts of fetuses of diabetic mothers. Epicardial attachment to the myocardium is critical to epicardial cell proliferation and formation of the epicardium

(31). The current study shows that pregestational diabetes inhibits epicardial development likely through an interruption of epicardial attachment to the myocardium and a reduction of epicardial cell proliferation. The number of epicardial cells undergoing apoptosis was low (0.3%), and no significant difference was observed at E12.5 between control and the offspring of diabetic mice. However, whether pregestational diabetes increases epicardial cell apoptosis in the offspring at other stages of development remains to be determined.

Epicardial EMT is a critical process in coronary artery development (32). In the current study, we demonstrate that pregestational diabetes decreases epicardial EMT. This is supported by the following experimental data. First, the number of Wt1⁺ cells, which are EPDCs from epicardial EMT, was reduced in the subepicardial space and in the compact myocardium in the offspring of diabetic mice. Second, high glucose levels inhibited epicardial cell outgrowth in cultured heart explants, and third, fate mapping analysis revealed a significant reduction of Wt1⁺ cell lineage in the fetal hearts of pregestational diabetic dams. The *Wt1*^{CreERT2} line has been shown to label the epicardium and its derivatives (33). The decreased

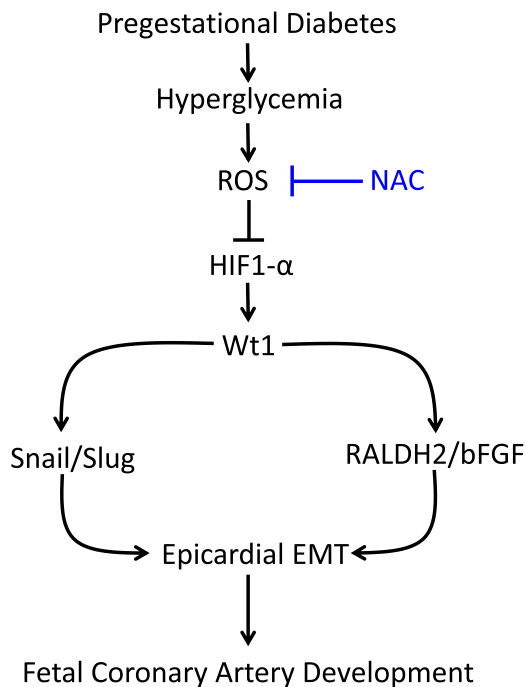


Figure 7—Schematic summary of ROS signaling on coronary artery malformation in the offspring of pregestational diabetic mice. Pregestational diabetes increases ROS through hyperglycemia. ROS production inhibits HIF-1 α and Wt1 expression in the fetal heart. Downregulation of Wt1 decreases epicardial EMT and results in coronary artery malformation through inhibition of Snail/Slug and RALDH2/bFGF pathways. All these abnormalities were prevented by treatment with NAC in the diabetic dams.

Wt1⁺ lineage in fetal hearts is consistent with our hypothesis that pregestational diabetes impairs epicardial EMT. To our knowledge, this is the first experimental evidence to show that pregestational diabetes inhibits epicardial EMT in the fetal heart.

HIF-1 α is a transcription factor that promotes vasculogenesis during embryonic development (34). To this end, HIF-1 α signaling has been shown to regulate epicardial EMT and EPDC migration into the myocardium, both of which are critical in patterning the coronary vasculature during early cardiac vasculogenesis (27). The effects of HIF-1 α are mediated by the expression of factors essential for coronary artery development, including Wt1 (17,35). Importantly, HIF-1 α is also ROS sensitive. Although low levels of ROS increase HIF-1 α expression and promote cardiovascular differentiation, high levels of ROS may inhibit HIF-1 α activity by inhibiting the binding of coactivator p300 to HIF-1 α (36,37). Furthermore, diabetes increases ROS levels through hyperglycemia and decreases the expression and activity of HIF-1 α (38,39). In the current study, ROS levels were significantly increased, whereas HIF-1 α expression and the number of Wt1⁺ epicardial cells and EPDCs were decreased in the hearts of embryos of pregestational diabetic mice. Of note, these changes were abrogated by NAC treatment, which reduces ROS levels in the embryonic heart. The

data suggest that pregestational diabetes impairs the HIF-1 α /Wt1 signaling pathway through elevated ROS levels in the fetal heart (Fig. 7).

Wt1 has been shown to regulate epicardial EMT through the expression of its downstream targets of Snail1, Slug, and RALDH2 (40–42). In line with our observation of reduced epicardial EMT, we further demonstrate that the expression of Snail1 and Slug is decreased in the embryonic hearts of pregestational diabetic mice. Retinoic acid feeds into an essential signaling pathway crucial for epicardial formation, epicardial attachment to the myocardium, myocardial growth and proliferation, and coronary artery development (43,44). bFGF is an important mediator in retinoic acid signaling that promotes epicardial EMT and vasculogenesis in the embryonic heart. The current results show that the expression levels of *Aldh1a2*, which encodes RALDH2, and its downstream target bFGF were diminished, suggesting impaired retinoic acid signaling in the fetal hearts of diabetic mothers. Thus, pregestational diabetes impairs both Wt1/Snail/Slug and Wt1/RALDH2/bFGF signaling pathways, which may contribute to decreased epicardial EMT and malformation of coronary arteries in the fetal heart (Fig. 7).

Under physiological conditions, ROS signaling regulates vasculogenesis (45). Although basal endogenous ROS levels are critical to normal vascular development, excessive ROS production during embryogenesis may impair vasculogenesis. In this regard, oxidative stress induced by maternal diabetes impairs vascularization in the yolk sac of rat embryos (46). NAC is a precursor of cysteine and decreases ROS levels through increases in GSH synthesis and antioxidant capacity (47). The current study shows that ROS and oxidative stress are increased in the fetal hearts of mice with pregestational diabetes. Of note, NAC treatment in diabetic females during gestation diminished ROS levels and restored expression of critical factors essential for epicardial growth and EMT. Importantly, NAC treatment rescued coronary artery malformation induced by pregestational diabetes. This study suggests a critical role of elevated ROS and its signaling in mediating coronary artery malformation in pregestational diabetes. However, whether NAC treatment normalizes GSH levels in fetal hearts is not known because GSH levels were not determined and other effects of NAC beyond ROS reductions cannot be excluded. Of note, antioxidant treatments prevent congenital heart defects induced by hyperglycemia or pregestational diabetes (20,48–50). The results are consistent with our recent findings that elevated ROS levels contribute to the abnormal development of congenital heart defects in the offspring of mice with pregestational diabetes, which is rescued by NAC treatment (20). Thus, NAC may have therapeutic potential in the prevention of congenital heart defects, including coronary artery malformation, in the offspring of mothers with pregestational diabetes.

In conclusion, the current study demonstrates that pregestational diabetes impairs epicardial EMT and

coronary artery development in mice. These abnormalities are associated with increased ROS production and decreased HIF-1 α /Wt1 signaling (Fig. 7). Of note, these abnormalities were all prevented by NAC treatment, suggesting a key role of ROS signaling in the malformation of coronary arteries resulting from pregestational diabetes. The coronary artery phenotype observed in the current study simulates human hypoplastic coronary artery disease, which carries a high risk of spontaneous myocardial infarction and sudden cardiac death (6). The current study suggests that pregestational diabetes could cause hypoplastic coronary arteries in mice. However, further clinical studies are required to determine whether pregestational diabetes increases the incidence of hypoplastic coronary artery disease in humans.

Funding. This study was supported by grant 000505 to Q.F. from the Heart and Stroke Foundation of Canada. Q.F. is a Heart and Stroke Foundation of Canada Career Investigator.

Duality of Interest. No potential conflicts of interest relevant to this article were reported.

Author Contributions. H.M. contributed to the research design, experiments, data analysis, and drafting and revision of the manuscript. X.L. contributed to the research design, experiments, data analysis, and revision of the manuscript. M.L. contributed to the experiments. Q.F. contributed to the study concept and research design, interpretation of the results, and revision of the manuscript. H.M. and Q.F. are the guarantors of this work and, as such, had full access to all the data in the study and take responsibility for the integrity of the data and the accuracy of the data analysis.

References

- Correa A, Gilboa SM, Besser LM, et al. Diabetes mellitus and birth defects. *Am J Obstet Gynecol* 2008;199:237.e1–237.e9
- Jenkins KJ, Correa A, Feinstein JA, et al.; American Heart Association Council on Cardiovascular Disease in the Young. Noninherited risk factors and congenital cardiovascular defects: current knowledge: a scientific statement from the American Heart Association Council on Cardiovascular Disease in the Young; endorsed by the American Academy of Pediatrics. *Circulation* 2007;115:2995–3014
- Garne E, Loane M, Dolk H, et al. Spectrum of congenital anomalies in pregnancies with pregestational diabetes. *Birth Defects Res A Clin Mol Teratol* 2012;94:134–140
- Lisowski LA, Verheijen PM, Copel JA, et al. Congenital heart disease in pregnancies complicated by maternal diabetes mellitus. An international clinical collaboration, literature review, and meta-analysis. *Herz* 2010;35:19–26
- Liu Y, Lu X, Xiang FL, et al. Nitric oxide synthase-3 deficiency results in hypoplastic coronary arteries and postnatal myocardial infarction. *Eur Heart J* 2014;35:920–931
- De Giorgio F, Abbate A, Stigliano E, Capelli A, Arena V. Hypoplastic coronary artery disease causing sudden death. Report of two cases and review of the literature. *Cardiovasc Pathol* 2010;19:e107–e111
- Laux D, Bessières B, Houyel L, et al. Early neonatal death and congenital left coronary abnormalities: ostial atresia, stenosis and anomalous aortic origin. *Arch Cardiovasc Dis* 2013;106:202–208
- Musiani A, Cernigliaro C, Sansa M, Maselli D, De Gasperis C. Left main coronary artery atresia: literature review and therapeutical considerations. *Eur J Cardiothorac Surg* 1997;11:505–514
- Madsen NL, Schwartz SM, Lewin MB, Mueller BA. Prepregnancy body mass index and congenital heart defects among offspring: a population-based study. *Congenit Heart Dis* 2013;8:131–141
- Pérez-Pomares JM, Macías D, García-Garrido L, Muñoz-Chápuli R. Contribution of the primitive epicardium to the subepicardial mesenchyme in hamster and chick embryos. *Dev Dyn* 1997;210:96–105
- Red-Horse K, Ueno H, Weissman IL, Krasnow MA. Coronary arteries form by developmental reprogramming of venous cells. *Nature* 2010;464:549–553
- Wu B, Zhang Z, Lui W, et al. Endocardial cells form the coronary arteries by angiogenesis through myocardial-endocardial VEGF signaling. *Cell* 2012;151:1083–1096
- Dettman RW, Denetclaw W Jr, Ordahl CP, Bristow J. Common epicardial origin of coronary vascular smooth muscle, perivascular fibroblasts, and intermyocardial fibroblasts in the avian heart. *Dev Biol* 1998;193:169–181
- Tian X, Hu T, Zhang H, et al. Subepicardial endothelial cells invade the embryonic ventricle wall to form coronary arteries. *Cell Res* 2013;23:1075–1090
- Pérez-Pomares JM, de la Pompa JL. Signaling during epicardium and coronary vessel development. *Circ Res* 2011;109:1429–1442
- Dunwoodie SL. The role of hypoxia in development of the mammalian embryo. *Dev Cell* 2009;17:755–773
- Wagner KD, Wagner N, Wellmann S, et al. Oxygen-regulated expression of the Wilms' tumor suppressor Wt1 involves hypoxia-inducible factor-1 (HIF-1). *FASEB J* 2003;17:1364–1366
- Moore AW, McInnes L, Kreidberg J, Hastie ND, Schedl A. YAC complementation shows a requirement for Wt1 in the development of epicardium, adrenal gland and throughout nephrogenesis. *Development* 1999;126:1845–1857
- Zhou B, Ma Q, Rajagopal S, et al. Epicardial progenitors contribute to the cardiomyocyte lineage in the developing heart. *Nature* 2008;454:109–113
- Moazzen H, Lu X, Ma NL, et al. N-acetylcysteine prevents congenital heart defects induced by pregestational diabetes. *Cardiovasc Diabetol* 2014;13:46
- Reece EA. Diabetes-induced birth defects: what do we know? What can we do? *Curr Diab Rep* 2012;12:24–32
- Yang P, Reece EA. Role of HIF-1 α in maternal hyperglycemia-induced embryonic vasculopathy. *Am J Obstet Gynecol* 2011;204:332.e1–332.e7
- Fine EL, Horal M, Chang TI, Fortin G, Loeken MR. Evidence that elevated glucose causes altered gene expression, apoptosis, and neural tube defects in a mouse model of diabetic pregnancy. *Diabetes* 1999;48:2454–2462
- Rerup CC. Drugs producing diabetes through damage of the insulin secreting cells. *Pharmacol Rev* 1970;22:485–518
- Liu Y, Lu X, Xiang FL, Lu M, Feng Q. Nitric oxide synthase-3 promotes embryonic development of atrioventricular valves. *PLoS One* 2013;8:e77611
- Mali VR, Palaniyandi SS. Regulation and therapeutic strategies of 4-hydroxy-2-nonenal metabolism in heart disease. *Free Radic Res* 2014;48:251–263
- Tao J, Doughman Y, Yang K, Ramirez-Bergeron D, Watanabe M. Epicardial HIF signaling regulates vascular precursor cell invasion into the myocardium. *Dev Biol* 2013;376:136–149
- Moss JB, Xavier-Neto J, Shapiro MD, et al. Dynamic patterns of retinoic acid synthesis and response in the developing mammalian heart. *Dev Biol* 1998;199:55–71
- Gittenberger-de Groot AC, Winter EM, Bartelings MM, Goumans MJ, DeRuiter MC, Poelmann RE. The arterial and cardiac epicardium in development, disease and repair. *Differentiation* 2012;84:41–53
- Liu Y, Feng Q. NOing the heart: role of nitric oxide synthase-3 in heart development. *Differentiation* 2012;84:54–61
- Olvey HE, Compton LA, Barnett JV. Coronary vessel development: the epicardium delivers. *Trends Cardiovasc Med* 2004;14:247–251
- Martínez-Estrada OM, Lettice LA, Essafi A, et al. Wt1 is required for cardiovascular progenitor cell formation through transcriptional control of Snail and E-cadherin. *Nat Genet* 2010;42:89–93
- Zhou B, Pu WT. Genetic Cre-loxP assessment of epicardial cell fate using Wt1-driven Cre alleles. *Circ Res* 2012;111:e276–e280
- Licht AH, Müller-Holtkamp F, Flamme I, Breier G. Inhibition of hypoxia-inducible factor activity in endothelial cells disrupts embryonic cardiovascular development. *Blood* 2006;107:584–590
- Lim J, Thiery JP. Epithelial-mesenchymal transitions: insights from development. *Development* 2012;139:3471–3486

36. Schmelter M, Ateghang B, Helmig S, Wartenberg M, Sauer H. Embryonic stem cells utilize reactive oxygen species as transducers of mechanical strain-induced cardiovascular differentiation. *FASEB J* 2006;20:1182–1184
37. Wang Y, Yang J, Yang K, et al. The biphasic redox sensing of SENP3 accounts for the HIF-1 transcriptional activity shift by oxidative stress. *Acta Pharmacol Sin* 2012;33:953–963
38. Ishizuka T, Hinata T, Watanabe Y. Superoxide induced by a high-glucose concentration attenuates production of angiogenic growth factors in hypoxic mouse mesenchymal stem cells. *J Endocrinol* 2011;208:147–159
39. Thangarajah H, Vial IN, Grogan RH, et al. HIF-1alpha dysfunction in diabetes. *Cell Cycle* 2010;9:75–79
40. Takeichi M, Nimura K, Mori M, Nakagami H, Kaneda Y. The transcription factors Tbx18 and Wt1 control the epicardial epithelial-mesenchymal transition through bi-directional regulation of Slug in murine primary epicardial cells. *PLoS One* 2013;8:e57829
41. Guadix JA, Ruiz-Villalba A, Lettice L, et al. Wt1 controls retinoic acid signalling in embryonic epicardium through transcriptional activation of Raldh2. *Development* 2011;138:1093–1097
42. von Gise A, Zhou B, Honor LB, Ma Q, Petryk A, Pu WT. WT1 regulates epicardial epithelial to mesenchymal transition through β -catenin and retinoic acid signaling pathways. *Dev Biol* 2011;356:421–431
43. Azambuja AP, Portillo-Sánchez V, Rodrigues MV, et al. Retinoic acid and VEGF delay smooth muscle relative to endothelial differentiation to coordinate inner and outer coronary vessel wall morphogenesis. *Circ Res* 2010;107:204–216
44. Lin SC, Dollé P, Ryckebusch L, et al. Endogenous retinoic acid regulates cardiac progenitor differentiation. *Proc Natl Acad Sci U S A* 2010;107:9234–9239
45. Zhou Y, Yan H, Guo M, Zhu J, Xio Q, Zhang L. Reactive oxygen species in vascular formation and development. *Oxid Med Cell Longev* 2013;2013:374963
46. Zabihi S, Eriksson UJ, Wentzel P. Folic acid supplementation affects ROS scavenging enzymes, enhances Vegf-A, and diminishes apoptotic state in yolk sacs of embryos of diabetic rats. *Reprod Toxicol* 2007;23:486–498
47. Samuni Y, Goldstein S, Dean OM, Berk M. The chemistry and biological activities of N-acetylcysteine. *Biochim Biophys Acta* 2013;1830:4117–4129
48. Roest PA, van Iperen L, Vis S, et al. Exposure of neural crest cells to elevated glucose leads to congenital heart defects, an effect that can be prevented by N-acetylcysteine. *Birth Defect Res A Clin Mol Teratol* 2007;79:231–235
49. Molin DG, Roest PA, Nordstrand H, et al. Disturbed morphogenesis of cardiac outflow tract and increased rate of aortic arch anomalies in the offspring of diabetic rats. *Birth Defects Res A Clin Mol Teratol* 2004;70:927–938
50. Morgan SC, Relaix F, Sandell LL, Loeken MR. Oxidative stress during diabetic pregnancy disrupts cardiac neural crest migration and causes outflow tract defects. *Birth Defects Res A Clin Mol Teratol* 2008;82:453–463

SUPPLEMENTARY DATA

Pregestational Diabetes Induces Fetal Coronary Artery Malformation via Reactive Oxygen Species Signaling

Hoda Moazzen, Xiangru Lu, Murong Liu, Qingping Feng

Department of Physiology and Pharmacology, University of Western Ontario, London, Ontario, Canada

Supplementary Table 1. Primer sequences for real time RT-PCR analysis.

Gene	Accession No.	Product Size	Primer Sequence (5'→ 3')
Aldh1a2	NM_009022.4	219	F: GGCAGCAATCGCTTCTCACA R: CAGCACTGGCCTTGGTTGAA
bFgf	NM_008006.2	174	F: CAAGGGAGTGTGTGCCAACC R: TGCCCAGTTCGTTTCAGTGC
Ctnnb1	NM_001165902.1	178	F: AGCTTCCTTTTTGGAAAGCTG R: CTTGGCTGAACCATCACAGAT
Snail1	NM_011427.2	114	F: CACACGCTGCCTTGTGTCT R: GGTCAGCAAAAAGCACGGTT
Slug	NM_011415.2	161	F: CAACGCCTCCAAGAAGCCCA R: GAGCTGCCGACGATGTCCAT
Hif-1 α	NM_010137.3	159	F: CTTGGACGCTCTGCCTATGA R: AGGTTGCGGGGGTTGTAGAT